Lattice dynamics of α-uranium

W. P. Crummett,* H. G. Smith, R. M. Nicklow, and N. Wakabayashi
Solid State Division, Oak Ridge National Laboratory, Oak Ridge, Tennessee 37830
(Received 26 January 1979)

The room-temperature lattice dynamics of α-uranium has been investigated. The phonon dispersion curves along the orthorhombic high-symmetry directions have been measured using inelastic neutron scattering techniques. The dispersion curves in the $[0\zeta 0]$ and $[00\zeta]$ directions are not very unusual. However, a depression and pronounced dips are observed in the $[\zeta 00]$ direction. The slopes of the long-wavelength acoustic branches are in agreement with the slopes predicted from the elastic constants. A four-neighbor Born–von Kármán general-tensor model, a 12-neighbor axially symmetric model, a simple shell model, and a simple Heine-Abarenkov pseudopotential model are unable to satisfactorily reproduce some of the $[\zeta 00]$ branches. However, a modified form of the shell model which includes forces to six neighbors is found to reproduce most of the branches well, including those in the $[\zeta 00]$ direction. A preliminary low-temperature experiment has revealed extra elastic scattering as well as significant phonon softening along the $[\zeta 00]$ direction.

I. INTRODUCTION

The α phase of uranium is stable at temperatures below 935 K, and several properties of this actinide metal indicate that the interatomic bonding in this phase is unusual. The structure of α-U is C-centered orthorhombic with two atoms in the primitive unit cell. (See Fig. 1.) The only other element found to possess this structure is cerium metal in a high-pressure phase stable above 56 kbars.[1] The elastic constants of α-U exhibit considerable anisotropy.[2] For example, the elastic constant C'_{11}, which represents the stiffness in any given direction in the crystal, displays maxima, minima, and saddle points for various directions in the three principal orthorhombic planes. Fisher has suggested that a strong maximum in the (100) plane and a minimum in the [010] direction are indicative of strong central force interactions with the first and fourth neighbors.[3] Van Ostenburg has made estimates of the magnitudes of the interatomic forces from the elastic constant data and a four-neighbor model.[4] However, there are in general many force constants in this model and it is impossible to establish the nature of the forces with elasticity data alone. A more detailed experimental description of the phonon dispersion curves is required.

X-ray- and neutron-diffraction studies have shown that the symmetry of α-U remains orthorhombic to at least 4 K,[5,6] but low-temperature anomalies in the elastic constants,[7,8] heat capacity,[9] and lattice parameters[10] are also indicative of the unusual nature of the bonding in α-U. As the temperature is decreased below room temperature the elastic constant C_{11} rises to a maximum at 256 K, then decreases to a sharp minimum at 43 K (perhaps a discontinuity) and displays hysteresis below this temperature. At 43 K there are anomalies in other elastic constants and a minimum in the atomic volume. Below 43 K the a and b lattice parameters increase with decreasing temperature, while the c parameter continues to decrease but more rapidly than it does above 43 K. The lattice parameters are continuous at 43 K and the net volume thermal expansion is negative below this temperature. Anomalies in the elastic constants and discontinuities in the lattice parameters have also been observed at 23 and 37 K and heat-capacity measurements have shown anomalies at 23, 37, and 43 K.

α-U exhibits additional unusual properties below 4 K. At zero pressure polycrystalline samples are found to be filamental superconductors with T_c above 1 K.[11] Bulk superconductivity is believed to begin at about 0.1 K in single crystals.[12] How-

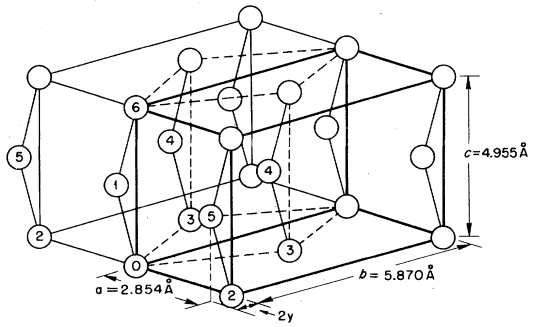

FIG. 1. C-centered orthorhombic structure of α-U. The orthorhombic unit cell is shown with bold lines and the dashed lines outline the primitive unit cell. The lattice parameters are those of 300 K and the y parameter is 0.1025 at this temperature. Some of the positions of the first six neighbors are also indicated.

ever, bulk superconductivity is enhanced under very modest pressure with a maximum T_c of 2.3 K occurring at 11 kbar.[13] It was first thought that the pressure dependence of T_c and the volume minimum might be associated with the occupancy of the $5f$ electronic states and the appearance of localized magnetic moments.[14] However, neutron-diffraction,[5] magnetic-susceptibility,[9,15] and recent heat-capacity measurements[12] are inconsistent with the formation of these moments. Nevertheless, the $5f$ electronic states are still thought to play a fundamental role in producing the peculiar superconducting[12,16] and other unusual properties of α-U, presumably through a mechanism which involves the bonding and the vibrational spectrum rather than through the formation of localized moments.

Since the lattice-dynamical properties are intimately related to the properties which show the anomalies outlined above, a thorough investigation of the lattice dynamics of α-U is desirable. In Sec. II we present the measurements of the room-temperature phonon dispersion curves of α-U. Previously reported measurements on α-U have been confined to the small wave-vector acoustic modes at temperatures near 43 K.[17] We also discuss the symmetry of all the branches in this section. The low symmetry of α-U makes the usual identification of the modes such as longitudinal acoustic, transverse optic, etc., ambiguous. The analysis of the dispersion curves with various models is reported in Sec. III and our conclusions are discussed in Sec. IV.

II. MEASUREMENTS AND RESULTS

The measurements were made on a triple-axis spectrometer at the Oak Ridge high-flux isotope reactor with various values of fixed outgoing energy E' ranging from 3.5 to 10 THz. Both "constant-Q" and "constant-E" scans were performed. The (002) planes of beryllium and graphite were used in various combinations as both monochromator and analyzer. For some of the measurements a pyrolytic graphite filter was employed. The Brillouin zone for α-U is shown in Fig. 2. Data were collected along the orthorhombic high-symmetry directions $[\zeta 00]$ (Σ), $[0\zeta 0]$ (Δ), and $[00\zeta]$ (Λ) on a single crystal with a volume of 0.1 cm^3. The results are presented in Table I and Fig. 3. As mentioned above there are two atoms in the primitive unit cell of α-U. The dynamical matrix is then a 6×6 complex matrix. In the Appendix we describe the results of the group-theoretical analysis we applied to classify the dispersion curves according to their symmetry. The data in Table I are labeled according to the symmetry notation described in this Appendix. In cases where there are two branches that belong to the same symmetry representation we have labeled the lower (upper) branch with the superscript 1 (2). The polarization vectors are also complex and may have components along more than one high-symmetry direction. The terms "longitudinal acoustic and optic" or "transverse acoustic and optic" are ambiguous; we will, however, occasionally use these terms to describe the dispersion curves but will also carefully identify the corresponding components of the polarization vectors.

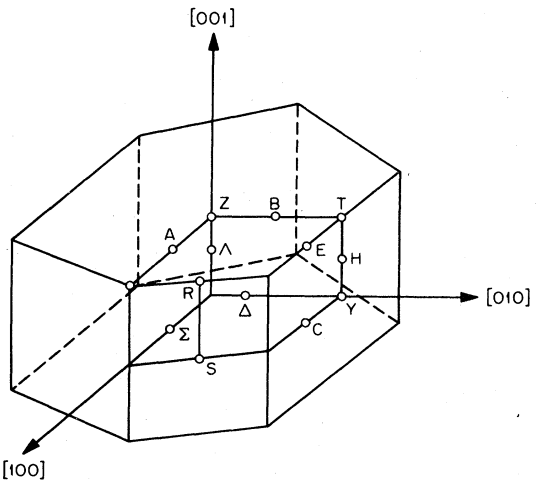

FIG. 2. First Brillouin zone for the C-centered orthorhombic lattice. Data were collected along the Σ, C, Δ, and Λ high-symmetry directions.

The slopes of the acoustic modes near $q=0$ are in agreement, within experimental errors, with those computed from the room-temperature elastic constants. The prominent features of the dispersion curves may be summarized as follows:

$[00\zeta]$ and $[0\zeta 0]$ Directions

The dispersion curves show no unusual features along the $[00\zeta]$ direction. The frequencies of the Λ_1 branches are solutions of a 2×2 submatrix in the block-diagonalized dynamical matrix for this direction and in principle do not cross. The polarization vectors of these branches correspond to mixtures of longitudinal acousticlike motions and transverse opticlike motions, the latter with atomic displacements along the [010] direction. The Λ_4 branches have polarization vectors which correspond to mixtures of transverse acousticlike and longitudinal opticlike motions. The Λ_2 and Λ_3 branches have atomic displacements along only the [100] direction.

The dispersion curves in the $[0\zeta 0]$ direction are also smooth across the Brillouin zone. There appears to be a broad minimum in the upper Δ_3

TABLE I. α-uranium phonon frequencies determined by inelastic neutron scattering.

Reduced wave vector	Frequency (10^{12} Hz)	Reduced wave vector	Frequency (10^{12} Hz)	Reduced wave vector	Frequency (10^{12} Hz)
Γ_1	3.12 ± 0.15			0.45	2.37 ± 0.10
		Σ_3		0.50	2.59 ± 0.05
Γ_5	3.59 ± 0.10	0.20	1.27 ± 0.05	0.55	2.68 ± 0.05
		0.30	1.63 ± 0.05	0.60	2.86 ± 0.10
Γ_7	2.46 ± 0.15	0.35	1.70 ± 0.05	0.70	3.14 ± 0.10
		0.40	1.80 ± 0.05	0.90	3.48 ± 0.10
Σ_1^1		0.45	1.91 ± 0.05	Y_4	3.53 ± 0.10
		0.50	2.01 ± 0.05		
0.05	0.57 ± 0.05	0.55	2.12 ± 0.05	Δ_1^1	
0.08	1.00 ± 0.05[a]	0.60	2.27 ± 0.05	0.10	0.60 ± 0.05[a]
0.123	1.40 ± 0.05[a]	0.65	2.44 ± 0.05	0.156	1.00 ± 0.05[a]
0.148	1.60 ± 0.05[a]	0.70	2.59 ± 0.05	0.20	1.14 ± 0.05
0.18	2.00 ± 0.05[a]	0.80	2.77 ± 0.05	0.25	1.45 ± 0.05
0.20	2.08 ± 0.10	0.90	2.90 ± 0.10	0.364	2.00 ± 0.05
0.25	2.10 ± 0.05	Y_8	2.96 ± 0.10	0.50	2.50 ± 0.15
0.30	2.24 ± 0.10			0.60	2.98 ± 0.15
0.40	2.14 ± 0.10			0.70	3.12 ± 0.15
0.45	1.99 ± 0.05	Σ_4^1		0.80	3.30 ± 0.10
0.50	2.02 ± 0.10	0.10	0.69 ± 0.05	0.90	3.32 ± 0.15
0.55	2.12 ± 0.10	0.15	1.01 ± 0.05	0.95	3.30 ± 0.25
0.60	2.24 ± 0.10	0.20	1.25 ± 0.05		
0.614	2.50 ± 0.10[a]	0.30	1.70 ± 0.05		
0.65	2.72 ± 0.06	0.35	1.50 ± 0.01	Δ_1^2	
0.70	2.72 ± 0.10	0.365[a]	1.80 ± 0.06	0.20	3.21 ± 0.15
0.75	3.05 ± 0.20	0.365[b]	1.52 ± 0.03	0.30	3.20 ± 0.15
0.80	2.79 ± 0.10	0.373	1.60 ± 0.06[a]	0.40	3.22 ± 0.15
0.85	2.74 ± 0.10	0.40	1.40 ± 0.20[a]	0.50	3.10 ± 0.10
0.90	2.46 ± 0.15	0.41	1.40 ± 0.10[a]	0.60	3.32 ± 0.10
0.95	2.27 ± 0.10	0.435	1.27 ± 0.03[b]	0.70	3.17 ± 0.10
Y_6	2.28 ± 0.10	0.45	1.06 ± 0.10	0.80	3.32 ± 0.15
		0.475	1.01 ± 0.10	0.90	3.46 ± 0.15
		0.50	1.06 ± 0.10		
Σ_1^2		0.535	1.18 ± 0.03[b]		
	3.18 ± 0.15	0.54	1.46 ± 0.03[b]	Δ_3^1	
0.20	3.14 ± 0.15	0.55	1.30 ± 0.10	0.30	1.27 ± 0.05
0.25	3.18 ± 0.10	0.56	1.40 ± 0.10[a]	0.40	1.65 ± 0.05
0.30	3.17 ± 0.15	0.60	1.60 ± 0.06[a]	0.50	1.95 ± 0.05
0.35	3.09 ± 0.15	0.62	1.71 ± 0.03[b]	0.60	2.28 ± 0.05
0.40	3.08 ± 0.20	0.635	1.80 ± 0.03[a]	0.70	2.52 ± 0.05
0.50	3.17 ± 0.10	0.65	2.00 ± 0.07[a]	0.80	2.70 ± 0.10
0.55	3.23 ± 0.10	0.675	2.20 ± 0.10[a]		
0.60	3.30 ± 0.10	0.70	2.39 ± 0.05		
0.70	3.26 ± 0.15	0.75	2.55 ± 0.05	Δ_3^2	
0.80	3.40 ± 0.20	0.80	2.55 ± 0.05	0.10	3.55 ± 0.15
0.90	3.40 ± 0.02	0.85	2.50 ± 0.15	0.20	3.40 ± 0.20
1.00	3.34 ± 0.10	0.95	2.49 ± 0.10	0.25	3.30 ± 0.20
		Y_7	2.49 ± 0.10	0.35	3.25 ± 0.15
				0.40	3.32 ± 0.15
Σ_2				0.55	3.10 ± 0.15
0.10	3.56 ± 0.15	Σ_4^2		0.70	3.00 ± 0.20
0.20	3.40 ± 0.20	0.10	2.42 ± 0.10	0.80	3.06 ± 0.15
0.30	3.15 ± 0.15	0.15	2.50 ± 0.10	0.90	3.06 ± 0.20
0.40	2.90 ± 0.10	0.20	2.46 ± 0.10	0.95	3.10 ± 0.15
0.60	2.70 ± 0.10	0.25	2.48 ± 0.08		
0.70	2.68 ± 0.10	0.28	2.20 ± 0.08[a]		
0.80	3.05 ± 0.15	0.30	2.32 ± 0.10		
0.95	3.18 ± 0.10	0.325	2.00 ± 0.07[a]		
Y_5	3.19 ± 0.15	0.35	1.90 ± 0.01		
		0.40	2.10 ± 0.10		

TABLE I. (*Continued*)

Reduced wave vector	Frequency (10^{12} Hz)	Reduced wave vector	Frequency (10^{12} Hz)	Reduced wave vector	Frequency (10^{12} Hz)
Δ_4^1		0.30	2.14 ± 0.10	Λ_3^2	
0.20	0.70 ± 0.05	0.35	2.34 ± 0.05	0.05	2.50 ± 0.15
0.30	1.00 ± 0.05	0.40	2.52 ± 0.05	0.10	2.50 ± 0.20
0.35	1.12 ± 0.05	0.45	2.38 ± 0.05	0.20	2.45 ± 0.10
0.40	1.30 ± 0.05	Z_1^1	2.20 ± 0.05	0.30	2.34 ± 0.10
0.50	1.54 ± 0.05			0.40	2.06 ± 0.10
0.60	1.83 ± 0.05	Λ_1^2			
0.70	2.00 ± 0.05	0.10	3.10 ± 0.10	Λ_4^1	
0.80	2.15 ± 0.10	0.20	2.98 ± 0.15	0.20	1.02 ± 0.05
0.90	2.23 ± 0.10	0.35	2.73 ± 0.10	0.30	1.44 ± 0.05
0.95	2.30 ± 0.10	0.40	2.60 ± 0.10	0.40	1.82 ± 0.05
Δ_4^2		0.45	2.80 ± 0.10	0.45	2.02 ± 0.05
0.10	2.54 ± 0.10	Z_1^2	2.96 ± 0.15	Λ_4^2	
0.20	2.50 ± 0.10			0.10	3.66 ± 0.15
0.35	2.42 ± 0.10	Λ_3^1		0.20	3.53 ± 0.15
0.40	2.46 ± 0.15	0.20	0.82 ± 0.02	0.30	3.50 ± 0.15
0.50	2.42 ± 0.10	0.30	1.23 ± 0.05	0.40	3.25 ± 0.10
0.70	2.38 ± 0.10	0.40	1.55 ± 0.05	0.45	3.16 ± 0.10
0.85	2.40 ± 0.10	0.45	1.72 ± 0.10		
		Z_2	1.88 ± 0.10		
Λ_1^1					
0.10	0.73 ± 0.10				
0.12	1.00 ± 0.03[a]				
0.22	1.60 ± 0.05[a]				

[a] Constant-E scans.
[b] Diagonal scans.

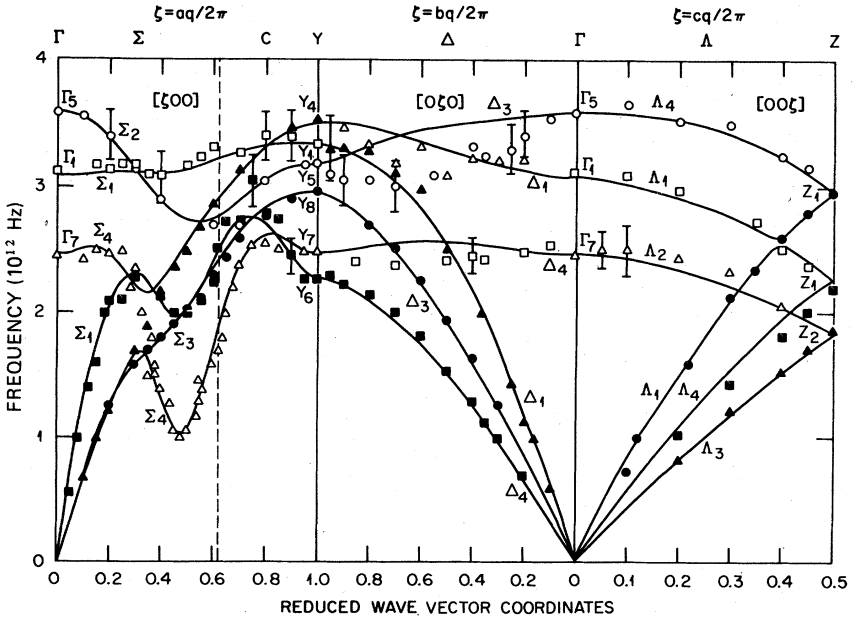

FIG. 3. Phonon dispersion curves of α-U. The solid lines are calculated from a six-neighbor modified shell model with axially symmetric interactions. The vertical dashed line in the [ζ00] direction indicates the Brillouin-zone boundary.

branch near $\zeta = 0.75$. The Δ_1 branches have atomic displacements along the [010] direction while the Δ_3 and Δ_4 branches have, respectively, [001] and [100] displacements. The phonon peak intensities in the scans of the upper (opticlike) Δ_1 and Δ_3 branches were usually very weak and the measurements of these branches were the most difficult in the experiment. The scatter in the data points probably reflects this difficulty.

[ζ00] Direction

The dispersion curves in this direction are the most unusual ones observed in α-U. There are pronounced dips in the lower Σ_1 and Σ_4 branches, and a slight depression in the Σ_3 branch. The Σ_2 branch displays considerable dispersion with a broad minimum. The pronounced dips and depression are centered at a ζ of about 0.475. The most pronounced dip is in the lower Σ_4 branch. The frequencies of the Σ_4 branches are also solutions of a 2×2 submatrix of the dynamical matrix and are, therefore, shown as branches which do not cross. The data indicate, however, that the splitting between the branches is small. The polarization vectors of these branches correspond to mixtures of transverse acousticlike motions with atomic displacements along the [010] direction and longitudinal opticlike motions. The open triangles represent modes which appear to be primarily longitudinal opticlike, while the solid triangles represent modes which are mostly transverse acousticlike. The opticlike modes were easily observable with Q values with the (220) and (201) reciprocal-lattice points. The majority of the data comprising this dip was collected with constant-E scans. Some representative constant-E scans are shown in Fig. 4. Two peaks in the neutron data at low and high ζ values were easily resolvable at phonon energies between 1.4 and 2.2 THz. Below 1.4 THz constant-Q scans and diagonal scans, in which both energy transfer and Q are varied, were more successful for the observation of this branch.

The polarization vectors of the upper Σ_1 branch appear to be mostly transverse opticlike, while the lower Σ_1 branch is primarily longitudinal acousticlike. The Σ_2 and Σ_3 branches are one-dimensional blocks of the dynamical matrix and represent transverse optic and acoustic modes, respectively, with polarization vectors along only the [001] direction.

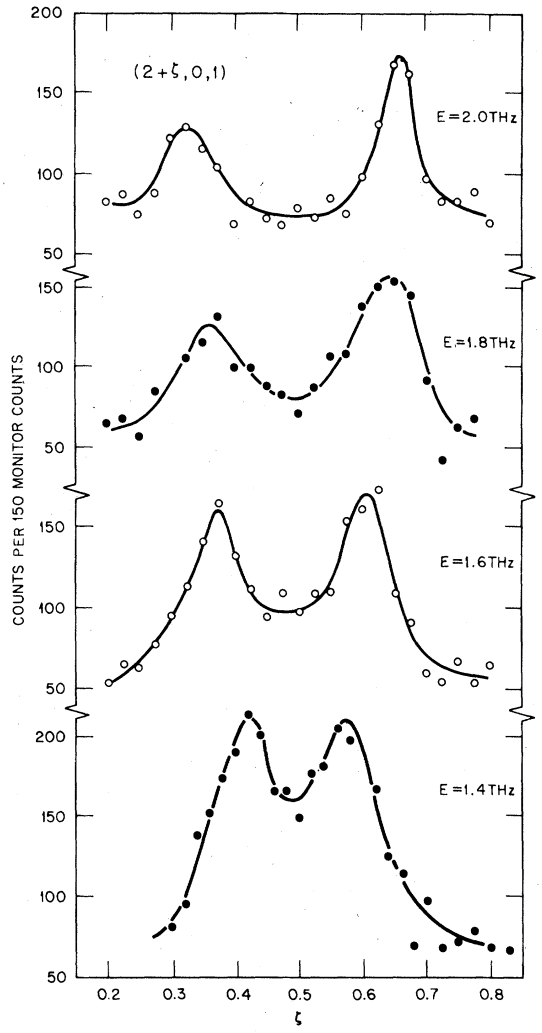

FIG. 4. Constant-E scans of the lower Σ_4 dispersion curve.

III. MODEL ANALYSIS

It is apparent from the dispersion curves that most of the difficulties in developing a model to adequately describe the lattice dynamics of α-U are associated with the [ζ00] data. A preliminary analysis of the range of the interatomic forces necessary to describe the dispersion curves in this direction was carried out. Since the α-U structure has a mirror plane perpendicular to the [100] direction, an expression for the sum of the squares of the lower and upper branches of either the Σ_1 or Σ_4 curves may be written

$$\nu_A^2(\zeta) + \nu_0^2(\zeta) = \sum_n \phi_n [1 - \cos(\eta \pi \zeta)] \ . \qquad (3.1)$$

$\nu_A(\zeta)$ [$\nu_0(\zeta)$] is the frequency of the lower [upper] branch and ϕ_n are the interplanar force constants which are linear combinations of the interatomic force constants. A least-squares fit of this expres-

sion to the Σ_1 and Σ_4 branches indicates that a minimum of four planes is necessary for a reasonable fit to the data. This implies that interactions to at least 11 neighbors are important. A simple Fourier series description of both the Σ_2 and Σ_3 branches is also possible. It is found that two planes are sufficient to fit the Σ_2 branch while three are necessary to describe the depression in the Σ_3 branch. The latter result emphasizes the importance of the eighth-neighbor interactions. The existence of a nonzero y-positional parameter prohibits the application of the Fourier analysis to the $[0\zeta 0]$ data. The $[00\zeta]$ data are smooth and the interplanar analysis was therefore not applied in this direction.

Since the eleventh neighbor occupies the position $(2a, 0, 0)$ the interplanar analysis of the Σ_1 and Σ_4 branches also illustrates that a large number of neighbors must be included even if we limit the real-space interactions to a comparatively short distance. Indeed, including force constants to only six neighbors in α-U corresponds to interactions with 18 atoms, all located less than 5 Å from the origin. In lattices with fcc and bcc symmetries, interactions with only second and third neighbors, respectively, involve this same number of atoms. Furthermore, the low symmetry of α-U gives rise to many independent Born–von Kármán force constants for each set of neighbors. For these reasons most of the models we applied to α-U employ axially symmetric force constants.

The $[00\zeta]$ data are reproduced well with a six-neighbor axially symmetric Born–von Kármán model. However, the agreement with the $[0\zeta 0]$ and the $[\zeta 00]$ data is poor. When axially symmetric forces to 11 neighbors are included, the agreement with the $[0\zeta 0]$ data is much better, although the Δ_3 branch is calculated to be somewhat higher than observed. In the $[\zeta 00]$ direction this model reproduces the Σ_2, Σ_3, and both Σ_4 branches well. The lower Σ_1 branch can also be reproduced satisfactorily but the upper Σ_1 branch is calculated to have a large dip, contrary to observation. Virtually no improvement in the fit is found when the first four neighbor forces are taken to be general tensor rather than axially symmetric.

To simulate polarization effects that may be present, the shell model has been applied to some of the transition metals, noble metals, and transition-metal carbides,[18,19] and we have applied it to α-U. This approach has been given some plausibility by microscopic theories, although these theories result in a more general form for the interatomic interactions of which the shell model is a special case.[19,20]

The form of the dynamical matrix for the shell model is

$$D = \overline{R} + Z^2 \frac{e^2}{v} \overline{C} - \left(\overline{T} + YZ \frac{e^2}{v} \overline{C}\right)\left(\overline{S} + \overline{K} + Y^2 \frac{e^2}{v} \overline{C}\right)^{-1}\left(\overline{T}^{\dagger} + YZ \frac{e^2}{v} \overline{C}\right), \tag{3.2}$$

where

$$\overline{R} = \overline{D} + 2\overline{F} + \overline{S}, \tag{3.3a}$$

$$\overline{T} = \overline{F} + \overline{S}, \tag{3.3b}$$

and $\overline{D}$, $\overline{F}$, and $\overline{S}$ are, respectively, the core-core, the different site core-shell, and the shell-shell interaction matrices. $\overline{K}$ is the single-site core-shell interaction matrix which in our calculations was taken to be diagonal and nonisotropic. Ye and Ze are the shell and ion charges, v is the volume of the primitive cell, and $\overline{C}$ is the screened Coulomb contribution. Since it is not clear how to evaluate the screened Coulomb coefficients, only the short-range terms were included in the majority of the calculations we will describe below.

In the simple shell model all the interactions are taken to act through the shells so that $\overline{R} = \overline{T} = \overline{S}$. However, in our calculations some core-shell overlap is permitted by introducing the parameter γ such that $\overline{S} = \gamma \overline{R}$. A simple axially symmetric shell model is able to reproduce the $[0\zeta 0]$ data better with fewer neighbors than the Born–von Kármán models, but the agreement with the $[\zeta 00]$ data is poor. While carrying out these calculations we noticed that for certain parameters and negative values of γ the term $(\overline{S} + \overline{K})$ becomes small for a limited q region. A dip can then be produced in the lower Σ_1 branch, while considerably less dispersion is calculated in the upper Σ_1 branch. This mechanism is similar to, but much simpler than, that of the double shell model.[19] The overall agreement with the dispersion curves was still not satisfactory, so we were motivated to allow $\overline{S}$ to be determined from a completely different set of parameters than was $\overline{R} = \overline{T}$. The form of the dynamical matrix is then

$$D = \overline{T} - \overline{T}(\overline{S} + \overline{K})^{-1}\overline{T}^{\dagger}. \tag{3.4}$$

The results of fitting a six-neighbor model of this type to the data are shown in Fig. 3. Most of the features of the dispersion curves are reproduced well, including the flat upper Σ_1 branch. The model does calculate a larger splitting than is observed between the Σ_4 branches at $\zeta = 0.35$ and the Σ_3 branch is still calculated slightly too high. However, the fit is far superior to that of any other model we applied to α-U. The quality of the fit is improved from a typical χ^2 value of

4.2 for a 12-neighbor Born–von Kármán model to 1.5 for this model.

This modified shell model contains 27 adjustable parameters, which is more than normally desirable for phenomenological models. However, the model contains only three more parameters than required by the much less successful 12-neighbor axially symmetric model. The axially symmetric bond stretching and bond bending parameters, the derived force constants, and the anisotropic core-shell coupling parameters for the fit shown in Fig. 3 are given in Table II. A decomposition of the contribution to the dispersion curves from each set of neighbors indicates that the second and fifth neighbors are primarily responsible for the dips in the lower Σ_1 and Σ_4 branches.

An attempt was also made to calculate the dispersion curves from a simple Heine-Abarenkov pseudopotential with free-electron random-phase approximation screening.[21,22] The pseudopotential forces are axially symmetric in this model. The reciprocal space sums were computationally very time consuming, and even when a convergence factor was employed, it was impossible to carry out a least-squares fitting calculation. Without a short-range Born–von Kármán contribution to the dynamical matrix, no set of pseudopotential parameters could be found which yielded all real frequencies along the $[\zeta 00]$ and $[0\zeta 0]$ directions. Parameters were found which gave all real frequencies along the $[00\zeta]$ direction, but the results were not nearly as satisfactory as those of the Born–von Kármán models.

IV. CONCLUSIONS

It was necessary to utilize a modified form of the shell model which employs a mechanism similar to that of the double shell model in order to satisfactorily reproduce the dispersion curves. As noted above, owing to the low symmetry of α-U, the real-space interaction range is comparatively short even when as many as 11 neighbors are included in the model calculation. Since the eleventh neighbor is only about 5.7 Å from the origin and since we have included general tensor forces for only the first four neighbors, we cannot conclude from the model calculations alone that the dips in the Σ_1 and Σ_4 branches are definitely anomalous. In fact, the most pronounced dip which appears in the lower Σ_4 branch was easily reproduced by the 11 neighbor axially symmetric Born–von Kármán model.

On the other hand the dips and depressions in the lower Σ branches are reminiscent of the anomalies observed in high T_c superconductors.[23] Their presence suggests that the electronic system may have a strong influence on the room-temperature lattice dynamics as well as the low-temperature (and high-pressure) mechanical properties. It has been proposed that the latter properties may be related to a softening of phonon modes[16] or possibly to the onset of a charge density wave.[24] The lower branches in the Σ direction are certainly congruous with both of these ideas.

Indeed, a preliminary low-temperature experiment has indicated that significant softenings of

TABLE II. Six-neighbor axially symmetric modified shell model force constants.

Neighbor	Interaction matrix	Bond stretching force constant (10^5 dyn/cm)	Bond bending force constant (10^5 dyn/cm)	ϕxx	ϕyy	ϕzz	ϕxy	ϕxz	ϕyz
1	T	−3.069	−4.450	−0.222	−0.472	−1.284	···	···	−0.515
	S	−3.074	0.181	0.090	−2.220	−1.226	···	···	−0.639
2	T	−1.102	−0.143	−0.551	−0.071	−0.071	···	···	···
	S	−0.464	0.624	0.232	0.312	0.312	···	···	···
3	T	−0.594	0.323	−0.043	−0.237	0.016	−0.123	···	···
	S	−0.710	−0.331	−0.201	−0.318	−0.165	−0.074	···	···
4	T	−0.960	0.035	−0.073	−0.116	−0.256	−0.110	−0.157	−0.191
	S	−1.905	0.125	−0.122	−0.209	−0.495	−0.224	−0.321	−0.389
5	T	−0.137	0.080	−0.016	0.030	−0.017	−0.011	−0.049	−0.010
	S	0.290	0.241	0.065	0.111	0.032	−0.011	−0.047	0.009
6	T	0.332	0.073	0.036	0.036	0.166	···	···	···
	S	0.075	0.457	0.229	0.229	0.037	···	···	···
	$K_{xx} = 3.862 \times 10^5$ dyn/cm								
	$K_{yy} = 4.352 \times 10^5$ dyn/cm								
	$K_{zz} = 1.493 \times 10^5$ dyn/cm								

the lower Σ_1 and Σ_4 branches occur, although the decreases in phonon frequencies begin at temperatures well above 43 K. For example, at 160 K the lower Σ_4 mode (LO-like) at $\zeta = 0.475$ has softened from 1.1 to 0.6 THz and the lower Σ_1 mode (LA-like) at $\zeta = 0.5$ has a frequency of 1.4 THz compared to 2.0 at room temperature. An elastic peak appears near (2.5, 2, 0) just above 60 K and grows in intensity as the temperature is decreased to 43 K and below. The width of this peak is within the instrumental resolution along both the [100] and [010] reciprocal space directions. It has been observed in several other Brillouin zones.

These results tend to emphasize the dependence of the lattice-dynamical properties on the details of the electronic system. Although there are currently very little data to which the results may be directly compared,[25] band-structure and Fermi-surface calculations have recently been undertaken for α-U.[24] The preliminary results included a calculation of the diagonal susceptibility function $\chi(\vec{Q})$, but there appears to be no structure in this function which could be responsible for dips in the Σ dispersion curves near $\zeta = 0.5$.[26] It is worth noting, however, that recent calculations for niobium indicate that a peak in $\chi(\vec{Q})$ is not necessary for electronically related dips to appear in the dispersion curves.[27]

Further low-temperature as well as high-pressure studies of the dispersion curves and elastic scattering are planned.

ACKNOWLEDGMENTS

The authors are grateful to G. H. Lander and E. S. Fisher of Argonne National Laboratory for the loan of the α-uranium crystal. The valuable experimental assistance of J. L. Sellers is also gratefully acknowledged. One of us (W.P.C.) wishes to express his appreciation to Oak Ridge Associated Universities for a Participantship from West Virginia University, Morgantown, West Virginia, during this work, to the Solid State Division, ORNL, for making his stay enjoyable and rewarding, and to C. A. Rotter of West Virginia University for many helpful discussions. Helpful conversations with W. Weber and A. J. Freeman are also gratefully acknowledged. Research was sponsored by the Division of Materials Sciences, U. S. Department of Energy under Contract No. W-7405-eng-26 with the Union Carbide Corporation.

APPENDIX

In this Appendix we present some results of the group-theoretical analysis of the lattice dynamics of α-U. The techniques of this analysis are well established and have been thoroughly reviewed.[28,29] The results are useful to classify the dispersion curves according to symmetry and to block diagonalize the dynamical matrix.

Insight into the nature of the atomic motions and the related neutron scattering structure factors associated with a particular dispersion curve may be obtained from the symmetry classifications. The space group of α-U is D_{2h}^{17} ($Cmcm$) and is nonsymmorphic. For the group-theoretical analysis it is convenient to take the atomic positions as $R_1 = (0, y, \frac{1}{4})$ and $R_2 = (0, -y, -\frac{1}{4})$, rather than those positions indicated in Fig. 1. The symmetry operators and matrix elements for the irreducible representations of the high-symmetry points and directions for α-U are tabulated by Kovalev.[30] The results of applying the projection-operator technique[28] to determine the polarization vectors are presented in Table III. θ_i's are functions of wave vector $\vec{q}$ which cannot be determined from the sym-

TABLE III. Polarization vectors determined by group-theoretical methods for some of the high-symmetry points and directions in α-U. The θ_i's are functions of $\vec{q}$ which cannot be determined from the symmetry analysis alone.

Γ_6 (100100)	Y_6 (100100)	Z_2^{11}, Z_2^{12} (100000)
Γ_7 (100$\bar{1}$00)	Y_7 (100$\bar{1}$00)	Z_2^{21}, Z_2^{22} (000100)
Γ_4 (010010)	Y_4 (010010)	Z_1^{11}, Z_1^{12} (0010$e^{i\theta_9}$10)
Γ_1 (0100$\bar{1}$0)	Y_1 (0100$\bar{1}$0)	Z_1^{21}, Z_1^{22} (01000$e^{i\theta_2}$)
Γ_8 (001001)	Y_8 (001001)	
Γ_5 (00100$\bar{1}$)	Y_5 (00100$\bar{1}$)	
Σ_1^1 (1, $e^{i\theta_3}$, 0, 1, $-e^{i\theta_3}$, 0)	Δ_4 (1, 0, 0, $e^{i\theta_5}$, 0, 0)	Λ_3 (1, 0, 0, 1, 0, 0)
Σ_4^1 (1, $e^{i\theta_4}$, 0, $\bar{1}$, $e^{i\theta_4}$, 0)	Δ_1 (0, 1, 0, 0, $e^{i\theta_6}$, 0)	Λ_2 (1, 0, 0, $\bar{1}$, 0, 0)
Σ_3^1 (0, 0, 1, 0, 0, 1)	Δ_3 (0, 0, 1, 0, 0, $e^{i\theta_7}$)	Λ_1 (0, $e^{i\theta_8}$, 1, 0, $-e^{i\theta_8}$, 1)
Σ_2^1 (0, 0, 1, 0, 0, $\bar{1}$)		Λ_4 (0, 1, $e^{i\theta_9}$, 0, 1, $-e^{i\theta_9}$)

TABLE IV. Compatibility relations derived from the character tables of the irreducible representations for the high-symmetry points and directions of α-U.

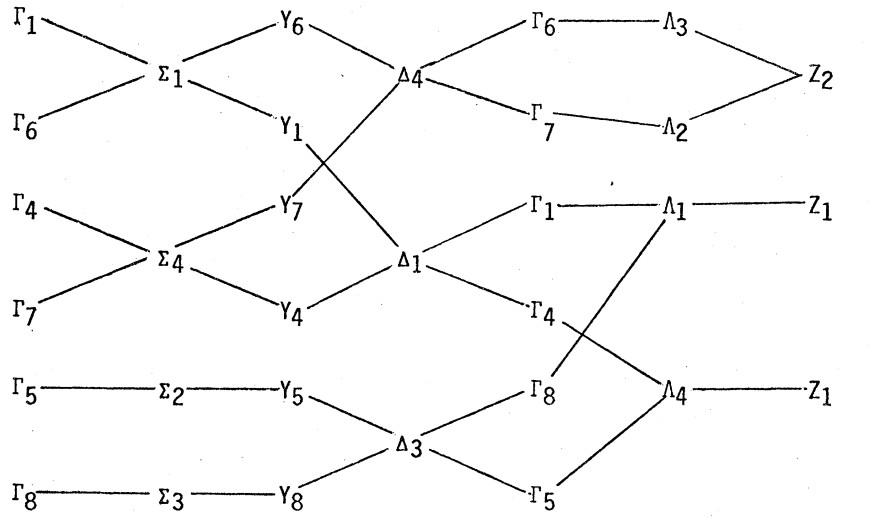

metry analysis alone.

At the Γ and Y points all the modes are purely longitudinal or transverse (i.e., the atomic displacements of each branch are along only one high-symmetry direction). In the [100] direction, only the Σ_2 and Σ_3 branches have associated atomic motions along a single principal direction (the [001] axis). The polarization vectors of the other branches have components along both the [100] and [010] directions. The Brillouin-zone boundary in this direction is not a point of higher symmetry than that of the Σ direction and the line C is a continuation of the [100] axis. The branches along Σ and C then have the same symmetry representations and we have chosen to label them only as Σ branches.

In the Δ direction the polarization vectors of each branch correspond to atomic displacements along the three principal directions, but the phases of the motions are not determined by the symmetry analysis. In the Λ direction the Λ_2 and Λ_3 branches have associated atomic motions along the [100] axis. The polarization vectors of the other branches in this direction have components along both [010] and [001] directions.

The compatibility relations are useful to visualize the continuities of the dispersion curves. These relations have been derived from the character tables of the irreducible representations and are summarized in Table IV.

The unitary matrix which block diagonalizes the dynamical matrix may be constructed from the results presented in Table III. For the three principal directions of α-U the largest block is of dimension two so that in the model analysis all of the phonon frequencies may be solved for analytically.

*Present address: Dept. of Physics, Montana State Univ., Bozeman, Mont. 59715.

[1]F. H. Ellinger and W. H. Zachariasen, Phys. Rev. Lett. 32, 773 (1974).
[2]E. S. Fisher and H. J. McSkimin, J. Appl. Phys. 29, 1473 (1958).
[3]E. S. Fisher, in *The Actinides: Electronic Structure and Related Properties*, edited by A. J. Freeman and J. B. Darby, Jr. (Academic, New York, 1974), Vol. II.
[4]D. O. Van Ostenburg, Phys. Rev. 123, 1157 (1961).
[5]C. S. Barrett, M. H. Mueller, and R. L. Hitterman, Phys. Rev. 129, 625 (1963).
[6]G. H. Lander and M. H. Mueller, Acta Crystallogr. B 26, 129 (1970).
[7]E. S. Fisher and H. J. McSkimin, Phys. Rev. 124, 67 (1961).
[8]E. S. Fisher and D. Dever, Phys. Rev. 170, 607 (1968).
[9]J. Crangle and J. Temporal, J. Phys. F 3, 1097 (1973).
[10]M. O. Steinitz, C. E. Burleson, and J. A. Marcus, J. Appl. Phys. 41, 5057 (1970).
[11]E. S. Fisher, T. H. Geballe, and J. M. Shreyer, J. Appl. Phys. 39, 4478 (1968).
[12]S. D. Bader, N. E. Phillips, and E. S. Fisher, Phys. Rev. 12, 4929 (1975).

[13]T. F. Smith and E. S. Fisher, J. Low Temp. Phys. 12, 631 (1973).
[14]T. H. Geballe, B. T. Matthias, K. Andres, E. S. Fisher, T. F. Smith, and W. H. Zachariasen, Science 152, 755 (1966).
[15]J. W. Ross and D. J. Lam, Phys. Rev. 165, 617 (1968).
[16]J. Wittig, Z. Phys. B 22, 139 (1975).
[17]J. M. Fournier, A. Delapalme, G. H. Lander, R. Pynn, N. Wakabayashi, and R. M. Nicklow, Bull. Am. Phys. Soc. 24, 275 (1978).
[18]W. Hanke, in *Proceedings of the International Conference on Phonons, Rennes, France*, edited by M. A. Nusimovici (Flammarion, Paris, 1972).
[19]W. Weber, Phys. Rev. B 8 5082 (1973).
[20]S. K. Sinha, R. P. Gupta, and D. L. Price, Phys. Rev. Lett. 26, 1324 (1971).
[21]W. Hanke and H. Bilz, in *Neutron Inelastic Scattering*, (IAEA Conf. Proc., Vienna, 1972), p. 3.
[22]M. Mostoller, Phys. Rev. B 5, 1260 (1972), and references therein.
[23]H. G. Smith, N. Wakabayashi, and M. Mostoller in *Superconductivity in d- and f-Band Metals*, edited by D. H. Douglass (Plenum, New York, 1976), p. 223.
[24]T. J. Watson-Yang, A. J. Freeman, and D. D. Koelling, Bull. Am. Phys. Soc. 23, 275 (1978).
[25]J. E. Shirber, A. J. Arko, and E. S. Fisher, Solid State Commun. 17, 553 (1975).
[26]A. J. Freeman (private communication).
[27]J. F. Cooke, Bull. Am. Phys. Soc. 23, 276 (1978).
[28]S. H. Chen, Phys. Rev. 163, 532 (1967).
[29]A. A. Maradudin and S. H. Vosko, Rev. Mod. Phys. 40, 1 (1968).
[30]O. V. Kovalev, *Irreducible Representations of the Space Groups*, translated from Russian by A. M. Gross (Gordon and Breach, New York, 1965).